PROCEEDINGS OF SPIE

SPIEDigitalLibrary.org/conference-proceedings-of-spie

Temperature-dependent absorption and gain of ytterbium-doped potassium double tungstates for chip-scale amplifiers and lasers

Yean-Sheng Yong, Shanmugam Aravazhi, Sergio A. Vázquez-Córdova, Jennifer L. Herek, Sonia M. García-Blanco, et al.

Yean-Sheng Yong, Shanmugam Aravazhi, Sergio A. Vázquez-Córdova, Jennifer L. Herek, Sonia M. García-Blanco, Markus Pollnau, "Temperature-dependent absorption and gain of ytterbium-doped potassium double tungstates for chip-scale amplifiers and lasers," Proc. SPIE 10106, Integrated Optics: Devices, Materials, and Technologies XXI, 1010606 (16 February 2017); doi: 10.1117/12.2252154

SPIE.

Event: SPIE OPTO, 2017, San Francisco, California, United States

Temperature-dependent absorption and gain of ytterbium-doped potassium double tungstates for chip-scale amplifiers and lasers

Yean-Sheng Yong[1,2], Shanmugam Aravazhi[1], Sergio A. Vázquez-Córdova[1,2], Jennifer L. Herek[2], Sonia M. García-Blanco[1,2], and Markus Pollnau[1,3]
[1]Integrated Optical Microsystems Group, MESA+ Institute for Nanotechnology, University of Twente, P.O. Box 217, 7500 AE Enschede, The Netherlands
[2]Optical Sciences Group, MESA+ Institute for Nanotechnology, University of Twente, P.O. Box 217, 7500 AE Enschede, The Netherlands
[3]Department of Materials and Nano Physics, School of Information and Communication Technology, KTH−Royal Institute of Technology, Electrum 229, Isafjordsgatan 22−24, 16440 Kista, Sweden

ABSTRACT

Ytterbium-doped potassium rare-earth double tungstate thin films are excellent candidates for highly efficient waveguide lasers, as well as high-gain waveguide amplifiers, with a record-high optical gain per unit length of 935 dB/cm recently demonstrated. However, the spectroscopic properties of these highly ytterbium-doped thin films and, in particular, their temperature dependence are not well investigated. These characteristics are required for the understanding of the behavior of the fabricated optical devices and crucial for further device optimization. We experimentally determined the absorption cross-sections for a potassium ytterbium gadolinium double tungstate, $KYb_{0.57}Gd_{0.43}(WO_4)_2$, thin film grown lattice matched onto an undoped $KY(WO_4)_2$ substrate. At room temperature, the peak cross-section value at 981 nm and the overall absorption spectrum are very similar to those of Yb-doped bulk potassium double tungstate crystals, although Yb is now the dominating rare-earth content. The temperature-dependent study shows a significant decrease of the absorption cross-section values at 933 nm and 981 nm with increasing temperature. We verify theoretically that this is due to the temperature dependence of fractional populations in the individual Stark levels of the absorbing crystal-field multiplet, in combination with the linewidth broadening with increasing temperature. Further investigations suggest that the broadening of absorption linewidth at 981 nm originates in the intra-manifold relaxation between the two lowest Stark levels of the ground state. Finally, the implications of the spectroscopic findings on the operating characteristics of waveguide amplifiers are investigated. Amplifiers operating at 80 °C are expected to exhibit only 67% of the maximum theoretical gain at room temperature.

Keywords: Rare-earth-doped materials, integrated optics materials, optical amplifiers, lasers, ytterbium

1. INTRODUCTION

Rare-earth-doped waveguide amplifiers and lasers are attractive for integrated optical systems, as a large number of active devices can be fabricated on the same chip and a straightforward flip-chip bonding process can be applied for the integration of active and passive modules. Nevertheless, the development of such chip-scale active devices has been lagging behind their semiconductor counterparts based on III-V compound materials for many years. Recently, a net gain of 935 dB/cm in ytterbium-doped potassium rare-earth double tungstate, $KRE(WO_4)_2:Yb^{3+}$ waveguide amplifiers operating without any active cooling was reported [1]. The gain achieved is two orders of magnitude higher than those of typical rare-earth-doped waveguide materials and comparable to those of semiconductor III-V devices (see [1, 2] and the references therein).

The outstandingly high gain per unit length of these $KRE(WO_4)_2:Yb^{3+}$ waveguide amplifiers is a result of thorough consideration on multiple important aspects. Firstly, active media doped with Yb^{3+} exhibit a simple energy-level scheme consisting of only the $^2F_{5/2}$ excited state and the $^2F_{7/2}$ ground state. Consequently, parasitic processes, such as energy-transfer upconversion, cross-relaxation, and excited-state absorption, which would limit the population inversion are absent. Secondly, the material gain of $KRE(WO_4)_2:Yb^{3+}$ is inherently higher due to its high transition cross-sections

Integrated Optics: Devices, Materials, and Technologies XXI, edited by Sonia M. García-Blanco, Gualtiero Nunzi Conti, Proc. of SPIE Vol. 10106, 1010606 · © 2017 SPIE
CCC code: 0277-786X/17/$18 · doi: 10.1117/12.2252154

which are superior to the ones of Yb^{3+}-doped yttrium aluminum garnet (YAG:Yb^{3+}) crystal [3-7]. Thirdly, a strategic lattice engineering approach [8, 9] is adopted for the growth of the active epitaxial layer on an undoped substrate of potassium yttrium double tungstate, $KY(WO_4)_2$, to simultaneously meet the requirements of a) maintaining lattice matching condition, b) increasing index of refraction, and c) maximizing the concentration of Yb^{3+}. Furthermore, with appropriate micro-structuring of the highly Yb^{3+}-doped $KRE(WO_4)_2$ layer (where RE = Gd, Lu, and/or Y), the resulting channel waveguides allow for high optical intensity to be maintained over a rather long interaction length, hence greatly enhance the light-matter interaction within a limited physical device length.

Though amplifier and laser experiments based on $KRE(WO_4)_2$:Yb^{3+} epitaxial layers with Yb^{3+} up to 47.5 at.% have been reported [1, 10-12], the actual spectroscopic properties, particularly the transition cross-sections, of such compound films remain unknown. In addition, it is well known that Yb^{3+}-doped solid-state amplifiers and lasers typically operate at elevated temperature due to conversion of the quantum defect, i.e., the energy difference between the pump and signal photons, to heat. Therefore, knowledge on the dependence of the transition cross-sections on temperature is necessary to understand and model the operational characteristics of these devices.

In this work, the transition cross-sections in $KRE(WO_4)_2$ thin films with 57 at.% Yb^{3+} concentration and their temperature dependence are investigated. It is found that the transition cross-sections of the epitaxial layers are very similar to the low-Yb^{3+}-concentration bulk crystals, despite the fact that Yb^{3+} is now the dominating rare-earth element. A strong temperature dependence of the peak absorption cross-sections is experimentally observed, which is related to the fractional populations in the individual Stark levels of the absorbing crystal-field multiplet as well as the absorption linewidth of the relevant transition. A simple model is derived to connect the two factors to the temperature dependence of the absorption cross-section. The results are in good agreement with the experimental data. Using the spectroscopic data obtained at room temperature and at 80 °C, the impact of elevated temperature to the gain performance is analyzed.

2. SAMPLE PREPARATION AND EXPERIMENTAL SETUP

The sample consists of a layer of $KYb_{0.57}Gd_{0.43}(WO_4)_2$ grown onto commercially available 1-mm-thick, **b**-oriented undoped $KY(WO_4)_2$ substrates (Altechna) by liquid-phase epitaxy using a $K_2W_2O_7$ solvent at 920−925 °C. In view of the high amount of Yb^{3+}, the lattice parameters of the epitaxial layer were engineered and optimized [8, 9] by co-doping with optically inert gadolinium (Gd) ions to minimize the lattice mismatch in the **a** and **c** crystallographic directions. The rear surface of the sample was lapped and polished to remove the excess growth layer, whereas the front surface of the sample was lapped and polished parallel to the substrate. The final thickness of the epitaxial layer was measured with a Dektak profilometer and found to be ~32 μm.

A dual-beam spectrophotometer (Shimadzu UV1800) with a spectral bandwidth of 1 nm is used together with a near-infrared (NIR) polarizer for the absorbance measurements. As the epitaxial layers were grown along the N_p direction, absorption spectra with $E||N_m$ and $E||N_g$ polarization can be measured. We limit our study to the absorption polarized to $E||N_m$, because this polarization exhibits the highest transition cross-sections and, therefore, is more commonly used for amplifier and laser experiments than the $E||N_g$ polarization. A series of measurements is performed while the polarizer is rotated by ~180° in steps to determine the sample orientation for absorption polarized to $E||N_m$. The absorption spectrum for each angle step is corrected for the spectral response of the polarizer at the same angle as well as the Fresnel reflections of the sample. The $E||N_m$ polarization is identified by the angle which produces the highest corrected absorption at the central absorption line near 981 nm wavelength. This peak absorption value follows a sinusoidal-like trend as the polarization angle is changed. The sample is mounted in a copper holder in contact with a Peltier element. The temperature of the sample is regulated using a thermoelectric temperature controller (Melcor MTTC1410).

3. RESULTS

The level energies of the bulk $KYb(WO_4)_2$, $KGd(WO_4)_2$:Yb^{3+}, and $KY(WO_4)_2$:Yb^{3+} crystals are very similar to each other [5, 7, 13], as shown in Fig. 1. Hence it is of interest to compare the spectroscopic properties of the $KYb_{0.57}Gd_{0.43}(WO_4)_2$ layer grown onto undoped $KY(WO_4)_2$ substrate to these bulk crystals. Figure 2(a) shows the effective absorption cross-section σ_{abs} in the $KYb_{0.57}Gd_{0.43}(WO_4)_2$ layer at 20 °C. It is determined from the measured absorption coefficient α and the Yb^{3+} concentration N_{Yb} of 3.8×10^{21} cm^{-3} using the expression

$$\sigma_{abs}(\lambda,T) = \alpha(\lambda,T)/N_{Yb}\,, \tag{1}$$

where λ represents the wavelength and T represents the temperature. The peak σ_{abs} value is 1.31×10^{-19} cm^2 near 981 nm wavelength. The spectrum is very comparable to those of bulk stoichiometric $KYb(WO_4)_2$ [13] and $KGd(WO_4)_2$:(1 at.%)Yb^{3+} [7] and in excellent agreement with that of $KY(WO_4)_2$:(~5 at.%)Yb^{3+} [5]. The reported peak σ_{abs} at ~981 nm for $KYb(WO_4)_2$, $KGd(WO_4)_2$:(1 at.%)Yb^{3+}, and $KY(WO_4)_2$:(~5 at.%)Yb^{3+} are 1.17×10^{-19} cm^2 [13], 1.16×10^{-19} cm^2 [7], and 1.33×10^{-19} cm^2 [5], respectively. The slight differences among the peak cross-section values considered here may be attributed to the spectral resolution of the different measurement systems and/or the measurement uncertainty of the doping concentration values. No abnormality is observed in the absorption of the epitaxial layer. This is in contrast to other Yb^{3+} hosts, such as LuAG and YAG, where color centers are apparent in as-grown samples especially at higher Yb^{3+} concentration [14, 15].

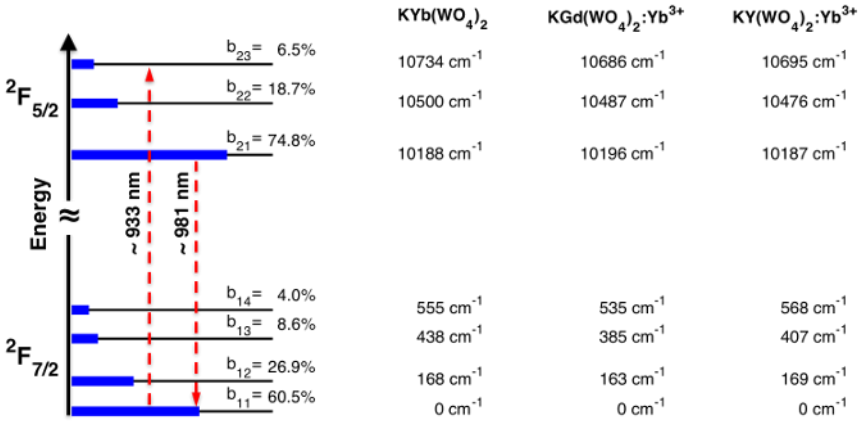

Figure 1. (a) Energy-level diagram of Yb^{3+} in various potassium rare-earth double tungstates [5, 7, 13]. The thick blue horizontal bars represent the estimated fractional populations within the manifolds at 300 K, calculated using the level energies of $KY(WO_4)_2$:Yb^{3+}. (Figure modified from [16].)

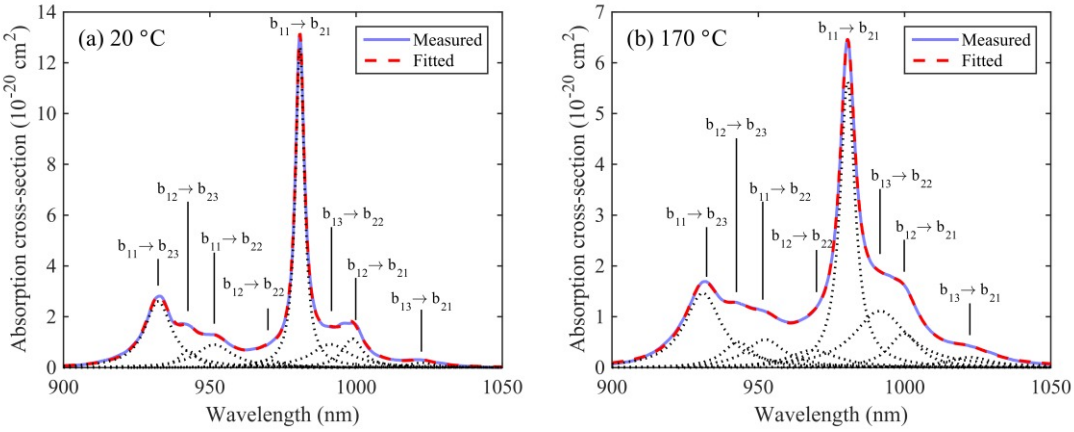

Figure 2. Experimentally determined effective absorption cross-section σ_{abs} in the $KYb_{0.57}Gd_{0.43}(WO_4)_2$ epitaxial film at (a) 20 °C and (b) 170 °C, shown together with the decomposed peaks corresponding to different Stark transitions. (Figure modified from [16].)

Figure 2(b) shows σ_{abs} at 170 °C, which is the highest temperature attainable with the Peltier element used in the experiment. With the increase of temperature, the magnitude of absorption at the central absorption line near 981 nm reduces rapidly. The wavelength corresponding to the peak is slightly blue-shifted from 980.8 nm at 20 °C to 980.5 nm at 170 °C. A similar, but less drastic, reduction of absorption is also noted at the peak near 933 nm. However, a larger shift of the corresponding peak wavelength for this transition is observed from 932.9 nm at 20 °C to 931.7 nm at 170 °C.

To further investigate the temperature dependence of the peak σ_{abs} at ~933 nm and ~981 nm, multiple-peak fitting is performed to decompose the absorption peaks using

$$\sigma_{abs}(\lambda,T)=\sum b_{1N}(T)\sigma_{atom}(\lambda,T), \tag{2}$$

where σ_{atom} represents the atomic cross-section. b_{1N} is the fraction of total population of the N-th Stark level within the ground-state manifold (where N = 1, 2, 3, or 4) relevant to the absorption transition, which can be estimated with the difference of energy with respect to the lowest Stark level, $E_{1N} - E_{11}$, the Boltzmann constant, k_B, and the temperature, T, using the following expression

$$b_{1N}(T)=\frac{\exp\left[-\left(E_{1N}-E_{11}\right)/k_BT\right]}{\sum_{j=1}^{4}\exp\left[-\left(E_{1j}-E_{11}\right)/k_BT\right]}. \tag{3}$$

An illustration of the distribution of the total population within the manifolds calculated at 300 K can be found in Fig. 1. Since the energy difference between the first and the second Stark level within the ground-state manifold is only ~165 cm^{-1}, a significant fraction of population is found at the second Stark level (N = 2) at room temperature ($k_BT \approx$ 200 cm^{-1}). Therefore, the change of temperature will lead to a significant effect on the absorption originating in the first Stark level (N = 1). Nevertheless, it is generally known that the absorption linewidth affects the peak absorption cross-section of the material as well, because the integral cross-sections remains the same [17]. As observed in Fig. 2, the linewidth of the decomposed peaks is broadened as the temperature is increased. To quantify the impact of these two factors on the measured absorption cross-section, we performed a fundamental analysis based on Eq. (2) (see [16] for the detailed analysis) and it is reasoned that the peak cross-section value of the major absorption peaks at 933 nm and 981 nm can be expressed by

$$\sigma_{abs}(T)\propto\frac{b_{11}(T)}{\Delta\nu(T)}, \tag{4}$$

where $\Delta\nu$ represents the relevant absorption linewidth. Hence, the absorption cross-section at any temperature can be determined from the cross-section value at a known temperature $\sigma_{abs}(T_0)$ using a simple model [16]

$$\sigma_{abs}(T)=\sigma_{abs}(T_0)\frac{b_{11}(T)}{b_{11}(T_0)}\frac{\Delta\nu(T_0)}{\Delta\nu(T)}. \tag{5}$$

Equation (5) indicates that the peak-absorption cross-section changes with temperature according to the temperature dependence of i) the Boltzmann factor of the starting Stark level and ii) the absorption linewidth of the relevant transition. This result is noteworthy as some reports in the literature estimate the change of absorption cross-section by only considering the Boltzmann factor [18].

Figure 3(a) shows the value of b_{11} at various temperatures, calculated based on the level energies of $KY(WO_4)_2$:Yb^{3+}. When the temperature increases from 20 °C to 170 °C, the value of b_{11} is reduced by ~18%. In other words, the ratio of b_{11}(170 °C)/b_{11}(20 °C) is ~0.82. Figure 3(b) displays the extracted $\Delta\nu$ of the decomposed absorption peaks near 933 nm and 981 nm. The corresponding ratio of $\Delta\nu$(20 °C)/$\Delta\nu$(170 °C) is ~0.73 and ~0.58 for the respective transitions at 933 nm and 981 nm. The change of the peak-absorption cross-sections at elevated temperatures with respect to 20 °C, $\sigma_{abs}(T)/\sigma_{abs}$(20 °C), is shown in Fig. 3(c). A reduction by ~40% and ~52% for the transitions near 933 nm and 981 nm, respectively, occurs. The result from the simple model of Eq. (5) is in good agreement with the measured reduction of peak magnitudes, demonstrating that the origin of the reduction of peak-absorption cross-section with temperature is a combination of the change in the population of the starting Stark level with temperature and the widening of the transition linewidth with temperature.

The measured linewidth $\Delta\nu$ is caused by intra-manifold transitions due to electron-phonon coupling on the fs time scale [17], which establishes the Boltzmann distribution. Considering a single-phonon contribution to the homogeneous broadening, i.e., the transition is accompanied by the absorption/emission of one phonon, a simplified expression can be derived from the detailed calculation of the electron-phonon interaction for non-adiabatic systems [19, 20],

$$\Delta\nu(T)\propto\left[\exp\left(\hbar\omega/k_BT\right)-1\right]^{-1}, \tag{6}$$

where $\hbar\omega$ is the energy of the phonon involved in the transition. This is the Bose-Einstein statistics applied to occupation of a phonon mode as a function of temperature. Applying Eq. (6) to the extracted linewidth at 981 nm given in Fig. 3(b), a least-squares fit provides $\hbar\omega$ = 164.3 ± 12 cm^{-1}, which corresponds to the energy gap between E_{12} and E_{11}.

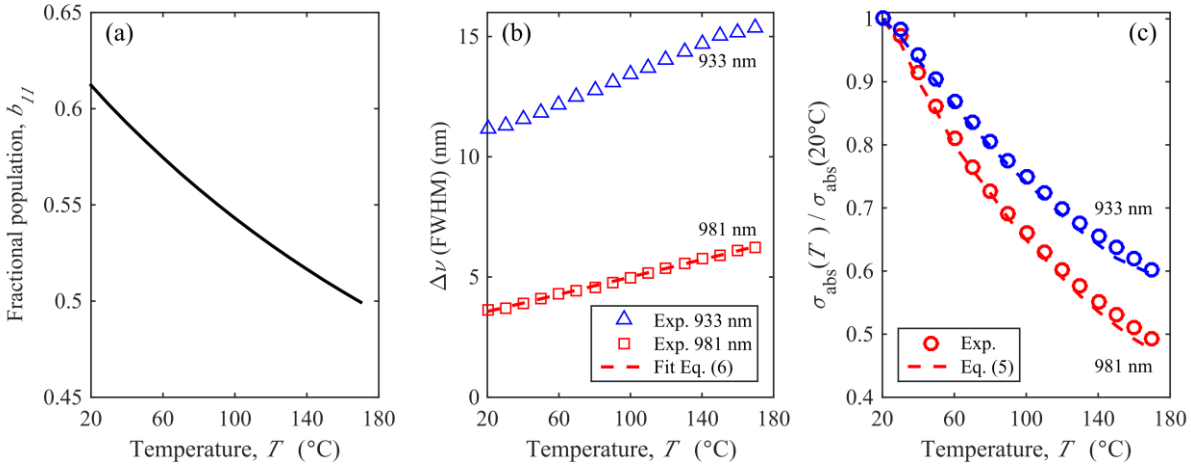

Figure 3. Spectroscopic data as a function of temperature: (a) calculated fractional population b_{11}, (b) extracted linewidth, $\Delta\nu$ of the absorption peaks near 933 nm and 981 nm and the fitted curve using Eq. (6), and (c) relative change of peak-absorption cross-section σ_{abs} of the transitions near 933 nm and 981 nm and the calculated curves using Eq. (5). (Figure taken from [16].)

The experimental data permits the estimation of gain performance at elevated temperature. Using the reciprocity method [21], the effective emission cross-section σ_{em} can be calculated. Subsequently, the gain cross-section can be readily estimated by considering σ_{abs}, σ_{em}, as well as the population inversion β as stated in Eq. 2 in [22]. With a pump wavelength of 933 nm, the maximum β is governed by the b_{11} and the b_{23} [12] (see Fig. 1). The maximum theoretical β at 20 °C is calculated as 90.7%, because at this excitation the pump transition becomes transparent. Assuming that the temperature is increased to 80 °C, the maximum β is lowered to 86.4%. The combination of the reduction of the maximum theoretical β and the decrease of the transition cross-sections leads to a reduction of the gain cross-section from 13.5×10^{-20} cm^2 at 20 °C to 9.1×10^{-20} cm^2 at 80 °C at 981 nm signal wavelength. In other words, the device operating at 80 °C is expected to exhibit 67% of the gain achievable at 20 °C.

4. CONCLUSIONS

The measured absorption data collected from a high-Yb^{3+}-concentration $KYb_{0.57}Gd_{0.43}(WO_4)_2$ epitaxial layer grown onto an undoped $KY(WO_4)_2$ substrate have been presented. The room-temperature absorption cross-section spectrum is found to be comparable to those reported for bulk materials. Temperature-dependent absorption measurements revealed a strong dependence of the major absorption peaks at 933 nm and 981 nm on temperature. With the aid of a simple model, the reduction of peak-absorption cross-section can be explained by two effects, the reduced fractional population of the relevant Stark level and the linewidth broadening. Further investigation on the magnitude of the extracted linewidths reveals that intra-manifold relaxation within the two lowest Stark levels plays a role in the broadening phenomenon for the central absorption line at 981 nm. It is shown that the temperature of the crystal has a significant influence on the optical gain.

REFERENCES

[1] Geskus, D., Aravazhi, S., García-Blanco, S. M., and Pollnau, M., "Giant optical gain in a rare-earth-ion-doped microstructure," Adv. Mater. 24(10), OP19-22, 2012.

[2] Pollnau, M., "Rare-earth-ion-doped channel waveguide lasers on silicon," IEEE J. Sel. Top. Quantum Electron. 21(1), 414-425, 2015.

[3] Koerner, J., Vorholt, C., Liebetrau, H., Kahle, M., Kloepfel, D., Seifert, R., Hein, J., and Kaluza, M. C., "Measurement of temperature-dependent absorption and emission spectra of Yb:YAG, Yb:LuAG, and Yb:CaF_2

between 20 °C and 200 °C and predictions on their influence on laser performance," J. Opt. Soc. Am. B 29(9), 2493-2502, 2012.
[4] Pujol, M. C., Bursukova, M. A., Güell, F., Mateos, X., Solé, R., Gavaldà, J., Aguiló, M., Massons, J., Díaz, F., Klopp, P., Griebner, U., and Petrov, V., "Growth, optical characterization, and laser operation of a stoichiometric crystal $KYb(WO_4)_2$," Phys. Rev. B 65(16), 165121, 2002.
[5] Kuleshov, N. V., Lagatsky, A. A., Podlipensky, A. V., Mikhailov, V. P., and Huber, G., "Pulsed laser operation of Yb-doped $KY(WO_4)_2$ and $KGd(WO_4)_2$," Opt. Lett. 22(17), 1317-1319, 1997.
[6] Mateos, X., Solé, R., Gavaldà, J., Aguiló, M., Massons, J., Díaz, F., Petrov, V., and Griebner, U., "Crystal growth, spectroscopic studies and laser operation of Yb^{3+}-doped potassium lutetium tungstate," Opt. Mater. 28(5), 519-523, 2006.
[7] Mateos, X., Pujol, M. C., Guell, F., Galan, M., Sole, R. M., Gavalda, J., Aguilo, M., Massons, J., and Diaz, F., "Erbium spectroscopy and 1.5-μm emission in $KGd(WO_4)_2$: Er,Yb single crystals," IEEE J. Quantum Electron. 40(6), 759-770, 2004.
[8] Pollnau, M., Romanyuk, Y. E., Gardillou, F., Borca, C. N., Griebner, U., Rivier, S., and Petrov, V., "Double tungstate lasers: From bulk toward on-chip integrated waveguide devices," IEEE J. Sel. Top. Quantum Electron. 13(3), 661-671, 2007.
[9] Aravazhi, S., Geskus, D., van Dalfsen, K., Vázquez-Córdova, S. A., Grivas, C., Griebner, U., García-Blanco, S. M., and Pollnau, M., "Engineering lattice matching, doping level, and optical properties of $KY(WO_4)_2$:Gd, Lu, Yb layers for a cladding-side-pumped channel waveguide laser," Appl. Phys. B 111(3), 433-446, 2013.
[10] Geskus, D., Aravazhi, S., Grivas, C., Wörhoff, K., and Pollnau, M., "Microstructured $KY(WO_4)_2$:Gd^{3+}, Lu^{3+}, Yb^{3+} channel waveguide laser," Opt. Express 18(9), 8853-8, 2010.
[11] Geskus, D., Aravazhi, S., Wörhoff, K., and Pollnau, M., "High-power, broadly tunable, and low-quantum-defect $KGd_{1-x}Lu_x(WO_4)_2$:Yb^{3+} channel waveguide lasers," Opt. Express 18(25), 26107-26112, 2010.
[12] Geskus, D., Bernhardi, E. H., van Dalfsen, K., Aravazhi, S., and Pollnau, M., "Highly efficient Yb^{3+}-doped channel waveguide laser at 981 nm," Opt. Express 21(11), 13773-13778, 2013.
[13] Klopp, P., Griebner, U., Petrov, V., Mateos, X., Bursukova, M. A., Pujol, M. C., Sole, R., Gavalda, J., Aguilo, M., Güell, F., Massons, J., Kirilov, T., and Diaz, F., "Laser operation of the new stoichiometric crystal $KYb(WO_4)_2$," Appl. Phys. B 74(2), 185-189, 2002.
[14] Luo, D., Zhang, J., Xu, C., Yang, H., Lin, H., Zhu, H., and Tang, D., "Yb:LuAG laser ceramics: a promising high power laser gain medium," Opt. Mater. Express 2(10), 1425-1431, 2012.
[15] Xu, X., Zhao, Z., Song, P., Zhou, G., Xu, J., and Deng, P., "Structural, thermal, and luminescent properties of Yb-doped $Y_3Al_5O_{12}$ crystals," J. Opt. Soc. Am. B 21(3), 543-547, 2004.
[16] Yong, Y. S., Aravazhi, S., Vázquez-Córdova, S. A., Carjaval, J. J., Díaz, F., Herek, J. L., García-Blanco, S. M., and Pollnau, M., "Temperature-dependent absorption and emission of potassium double tungstates with high ytterbium content," Opt. Express 24(23), 26825-26837, 2016.
[17] Eichhorn, M. and Pollnau, M., "Spectroscopic foundations of lasers: spontaneous emission into a resonator mode," IEEE J. Sel. Top. Quantum Electron. 21(1), 9000216, 2015.
[18] Balembois, F., Castaing, M., Georges, P., and Georges, T., "Line competition in an intracavity diode-pumped Yb:KYW laser operating at 981nm," J. Opt. Soc. Am. B 28(1), 115-122, 2010.
[19] Demirkhanyan, G. G., Demirkhanyan, H. G., Kokanyan, E. P., Kostanyan, R. B., Gruber, J. B., Nash, K. L., and Sardar, D. K., "Phonon effects on zero-phonon transitions between Stark levels in $NaBi(WO_4)_2$:Yb^{3+}," J. Appl. Phys. 105(6), 063106, 2009.
[20] Demirkhanyan, G. G. and Kostanyan, R. B., "Temperature dependence of spectral-line intensities in YAG:Yb^{3+}," Laser Phys. 18(2), 104-111, 2011.
[21] Payne, S. A., Chase, L. L., Smith, L. K., Kway, W. L., and Krupke, W. F., "Infrared cross-section measurements for crystals doped with Er^{3+}, Tm^{3+}, and Ho^{3+}," IEEE J. Quantum Electron. 28(11), 2619-2630, 1992.
[22] Yang, J., van Dalfsen, K., Wörhoff, K., Ay, F., and Pollnau, M., "High-gain Al_2O_3:Nd^{3+} channel waveguide amplifiers at 880 nm, 1060 nm, and 1330 nm," Appl. Phys. B 101(1), 119-127, 2010.